SYMPOSIUM
on
FLOW-INDUCED VIBRATIONS

VOLUME 1
EXCITATION AND VIBRATION OF BLUFF BODIES IN CROSS FLOW

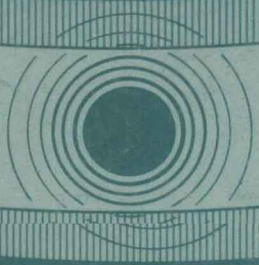

Editors
M.P. PAIDOUSSIS
O.M. GRIFFIN
M. SEVIK

SYMPOSIUM
on
FLOW-INDUCED VIBRATIONS

VOLUME 1
EXCITATION AND VIBRATION OF BLUFF BODIES IN CROSS FLOW

Presented at

THE ASME WINTER ANNUAL MEETING
NEW ORLEANS, LOUISIANA
DECEMBER 9-14, 1984

Symposium co-sponsored by

Applied Mechanics, Fluids Engineering, Heat Transfer, Noise Control and Acoustics, Nuclear Engineering, and Pressure Vessels and Piping Divisions

Sessions in this Volume co-sponsored by

FLUIDS ENGINEERING, APPLIED MECHANICS, AND NOISE CONTROL AND ACOUSTICS DIVISIONS

Edited by

M. P. PAIDOUSSIS (Principal Editor)
McGill University
Montreal, Quebec, Canada

O.M. GRIFFIN
Naval Research Laboratory
Washington, D.C.

M. SEVIK
David Taylor Naval Ship R & D Center
Bethesda, Maryland

THE AMERICAN SOCIETY OF MECHANICAL ENGINEERS
United Engineering Center 345 East 47th Street New York, N.Y. 10017

Library of Congress Catalog Card Number 84-72467

PREFACE

The 1984 ASME Symposium on Flow-Induced Vibration is a unique event in the annals of technical meetings organized by ASME. Apart from promising to be one of the most important symposia anywhere on this topic in recent memory (only time will tell exactly how important), it is the first time that such a large symposium on the subject has been organized by ASME. Furthermore, it is the first time that no less than six Divisions of the ASME have cooperated in co-sponsoring a symposium on any given subject, which surely bespeaks of the importance of the subject matter of this particular Symposium. The participating Divisions are:

Applied Mechanics, Fluids Engineering, Heat Transfer, Noise Control and Acoustics, Nuclear Engineering, and Pressure Vessels and Piping.

I should like to thank them all, for without their support this Symposium would not have been the success that it is promising to be.

The Proceedings of the Symposium are published in six bound volumes, containing sixty-eight papers in all, as follows:

Volume 1 Excitation and Vibration of Bluff Bodies in Cross Flow
Volume 2 Vibration of Arrays of Cylinders in Cross Flow
Volume 3 Vibration in Heat Exchangers
Volume 4 Vibration Induced by Axial and Annular Flows
Volume 5 Turbulence-Induced Noise and Vibration of Rigid and Compliant Surfaces
Volume 6 Computational Aspects of Flow-Induced Vibration

The organization of a Symposium of this size, with world-wide participation (from 12 countries), has been both a challenging and rewarding experience. It entailed a great deal of work by many people: the session developers, the reviewers, ASME Headquarters' staff, the 1984 WAM Organizers and, of course, the authors. Of the many people involved, too numerous to mention by name here, I am specially indebted to the session developers and co-editors (O. M. Griffin, M. Sevik, M. K. Au-Yang, S. -S. Chen, J. M. Chenoweth, M. D. Bernstein and A. J. Kalinowski), and would like to single out two: Dr. M. K. Au-Yang and Dr. S. -S. Chen, whom I would like to thank for their unswerving support from the very beginning, when the possibility of a "multidivisional symposium" looked like a pie in the sky! I would also like to thank my secretary, Ruth Gray, for efficiently handling the enormous amount of paperwork involved in several passes of sixty-eight-plus papers across my desk.

Michael P. Paidoussis
Principal Symposium Coordinator
and Principal Editor

FOREWORD

The dynamic response of a solitary bluff body in crossflow, the forces exerted on the body and the fluid mechanics of the flow around it have been studied very extensively and for a very long time, starting in earnest with Strouhal's work in 1878. Scientific fascination with the subject goes back to the time of Leonardo da Vinci, and even to the first mention in antiquity of the wind-induced vibration and sound of the Aeolian harp. However, despite the many advances and insights gained through the efforts of many researchers over the years, and despite the numerous conferences and symposia either largely or wholly devoted to flow-induced vibrations, there still remain questions to be answered and new facets to be explored. Thus researchers remain both interested and busy on this subject.

Not only is there interest on the dynamics of bluff bodies in cross-flow as a fundamental problem in fluid mechanics and fluid-elasticity, but there is also a great deal of interest from the viewpoint of engineering practice. Indeed, the scope of practical investigations is increasing as the subject becomes important in newer technological fields, while still retaining its importance in the older, traditional areas. Flow-induced vibrations of bluff bodies in cross-flow currently is important in wind engineering and structural design, naval and offshore technology, pressure vessel and piping design, and nuclear engineering, to name but a few. Each problem area brings its own set of peculiarities and special problems to the subject. For example, the behaviour of bluff bodies is different in dense fluids, as opposed to light fluids, and in two-phase flows, it is different in various ranges of the Reynolds number; it depends on the scale and level of the turbulence intensity; it is different when the separation points remain fixed during vibration (as with prismatic bluff bodies); it depends on whether body motions are large or small; and so on.

The fourteen papers in this volume give some idea of the wide spectrum of the various aspects and applications of flow-induced vibration. Some papers deal with the response of cylinders to vortex shedding; others with the turbulent buffeting of cylindrical and quasi-cylindrical bodies in wind or water currents, and with the suppression of the wind-induced motions; with the effects of high-turbulence cross-flow-induced forces and vibration; and with the presence of entrained air in liquid cross flows, in industrial environments.

On behalf of the Organizing Committee of this Symposium, we thank the authors for their cooperation in submitting papers of high quality on the topic of this Volume 1 of the Proceedings, Excitation and Vibration of Bluff Bodies in Cross-Flow. And we commend them for their willingness to participate and to share their experience with others who are interested in flow-induced vibrations. We also would like to thank the many reviewers for their thoughtful comments, which have contributed to the overall quality of the papers finally accepted for inclusion in the Symposium and its Proceedings.

M. P. Paidoussis

O. M. Griffin

M. Sevik

CONTENTS

VIBRATIONS AND FLOW-INDUCED FORCES CAUSED BY VORTEX SHEDDING

O. M. Griffin
Marine Technology Division
Naval Research Laboratory
Washington, D. C.

ABSTRACT

This paper discusses available data for vortex-induced lift, drag, and displacement amplitude from numerous experiments which have been conducted over the past several years. Recent measurements of the component of the overall lift force which drives the oscillations are compared with previously-reported data. There is good agreement which further confirms the complex behavior of the lift force as a circular cylinder undergoes vortex-induced vibrations. It is clear from the results that there is a limiting amplitude of vibration as the exciting force (and force coefficient C_{LE}) first increases from zero to a maximum (C_{LE} = 0.5 to 0.6) and then decreases again to zero as the limiting vibration amplitude (± 1 or more diameters) is approached. Recent measurements of the mean in-line drag forces on freely-vibrating cylinders have shown that the drag coefficient is amplified by as much as 250 percent in water at large vibration amplitudes near the limiting value. Drag force measurements with cylinders which were forced to vibrate under similar conditions yielded comparable results. For both the lift and drag measurements the Reynolds numbers were in the range Re = 10^3 to 10^4 and slightly higher. Thus the results are suitable in many practical applications for structures both in air and in water.

NOMENCLATURE

C_D, C_{D0}	Steady drag coefficient on a vibrating (stationary) cylinder or cable.
C_L	Lift coefficient; see Eq. (6).
C_{LE}	Excitation lift force coefficient; see Eq. (6).
D	Body diameter (m or ft).
f_n	Natural frequency in the fluid medium (Hz).
f_s	Strouhal frequency (Hz).
I_i	Modal scaling factor; see Eq. (4).
k_s	Reduced damping; see Eq. (1).
L	Body length (m or ft).
m	Cable physical mass per unit length (kg/m or lb_m/ft).
m'	Cable virtual mass (physical plus added mass) per unit length (kg/m or lb_m/ft).
P	Power transmission to the cylinder, $\bar{P}/\rho f^3 D^4$.
St	Strouhal number, $f_s D/V$.
V	Incident flow velocity (m/s or ft/sec).
V_r	Reduced velocity, $V/f_n D$.
w_r	Response parameter, $(1 + 2\,\bar{Y}/D)\,(V_r \mathrm{St})^{-1}$; see Eq. (10).
$\bar{y}$	Cross flow displacement (m or ft).
$\bar{Y}$	Cross flow displacement amplitude (m or ft).
Y	Normalized displacement amplitude, $\bar{Y}/D$.
$Y_{\mathrm{EFF,MAX}}$	Normalized displacement amplitude; see Eq. (4).
$\bar{z}$	Coordinate measurement along the cylinder or cable (m or ft).

δ	Log decrement of structural damping; see Eq. (1).
γ_i	Normalizing factor; see Eq. (4).
ϕ	Phase angle (deg. or rad); see Eq. (6).
μ	Mass ratio, $\rho D^2/8\pi^2 St^2 m$; see Eq. (2).
ν	Kinematic fluid viscosity (m^2/sec or ft^2/sec).
ρ	Fluid density (kg/m^3 or lb_m/ft^3).
$\psi_i(z)$	Mode shape for i th flexible beam mode; see Eq. (3)
ζ_s	Structural damping ratio; see Eq. (2).

INTRODUCTION

It is often found that bluff, or unstreamlined, structures display undesirable oscillatory instabilities arising from their motion relative to a surrounding fluid. A common mechanism for resonant, flow-excited oscillations is the organized and periodic shedding of vortices as the flow separates alternately from opposite sides of a long, bluff body. These vortices result in steady and unsteady drag forces in line with the flow and unsteady lift or side forces perpendicular to the flow direction. If the structure is flexible and lightly damped internally, then resonant oscillations can be excited normal or parallel to the incident flow direction. For the more common cross flow oscillations, the body and the wake usually oscillate in unison at a frequency near one of the characteristic frequencies of the structure. The shedding meanwhile is shifted away from the natural, or Strouhal, frequency at which pairs of vortices would be shed if the structure were restrained from oscillating. This phenomenon is known as "lock-on" or "wake capture."

The vortex-excited oscillations of marine cables, commonly termed *strumming*, result in increased steady and unsteady hydrodynamic forces, and amplified acoustic flow noise. They sometimes lead to early fatigue, structural damage and to failure. Flow-excited oscillations very often are a critical factor in the design of marine cable arrays, riser systems, and offshore platforms. Flow-induced vibrations also cause serious problems in nuclear reactors and reactor components. In air, chimney stacks, high-tension power lines and bus-bars commonly vibrate due to vortex shedding.

The dynamic analysis of structures and cable systems both in air and in water has become an important consideration in the prediction of stress distributions and fatigue lives. Reliable experimental data are now reasonably well in hand for the dynamic response characteristics and flow-induced forces on a model scale. Based upon these experiments, semi-empirical prediction models have been developed and favorably compared with field test data.

BASIC CHARACTER OF VORTEX SHEDDING

The frequency f_s of the vortex shedding from a circular cylinder is related to the other main flow parameters (D, the diameter of the cylinder; V, the flow velocity) through the nondimensional Strouhal number defined as

$$St = \frac{f_s D}{V}.$$

The value of the Strouhal number varies somewhat in different regimes of the Reynolds number and with the shape of the cylinder (circular, D-section, triangular, etc). For the range of the Reynolds number where the Strouhal number remains constant the relation between the shedding frequency and the velocity is linear for a given cylinder, i.e.

$$f_s = KV,$$

where $K = St/D$. If a cylinder immersed in a flowing fluid is free to oscillate in the cross-flow direction, then the latter relation does not hold in the vicinity of the natural frequency of the cylinder. This resonance phenomenon—called "lock-on" or "wake capture"—is discussed in this paper.

If the Reynolds number is lower than about 10^5, then the vortex shedding is predominantly periodic and the value of the Strouhal number can be assumed to be about 0.2 for a circular cylinder or cable. Measurements of the frequencies, displacement amplitudes and forces which result from vortex-excited oscillations have been obtained by many investigators from experiments both in air and in water. Fairly detailed reviews of the basic aspects of the problem of vortex-excited oscillations in general has been made recently by Sarpkaya [1] and Bearman [2]. King [3], and Griffin and Ramberg [4,5] have discussed the subject in the context of ocean engineering applications. Simmons and Cleary [6] Rawlins [7], and Adami and Batch [8] recently have discussed problems caused by vortex shedding from structures in air. Paidoussis [9] has discussed the problem of vortex-induced vibrations as one part of an extensive review of flow-induced vibration problems in reactors and reactor components.

AMPLITUDES OF DISPLACEMENT

A typical structure used for experimental vortex shedding studies consists of a cylinder placed normal to the flow and flexibly supported in some manner at each end. Representative measurements for such a cylinder in air have been reported by Griffin and Koopmann [10] and in water by Dean, Milligan and Wootton [11]. The results obtained are generally the same in both media. As the incident flow velocity V, or the "reduced velocity" V_r as in Fig. 1, is increased the unsteady displacement amplitude first builds up to a maximum, after which it begins to decrease as the upper limit of the resonance is approached. For one example shown in the figure the lock-on range, defined by vibration displacements greater than the resonant threshold (taken here as $2\bar{Y}/D = 0.1$), is given by reduced velocities between $V_r = 4.5$ and 7.5 in air, with the maximum of $\bar{Y}/D$ occurring at $V_r \sim 6$. For the in-water experiments the resonance range is somewhat wider, from $V_r = 4$ to nearly 8, but the peak value of $\bar{Y}/D$ again is excited at $V_r \sim 6$.

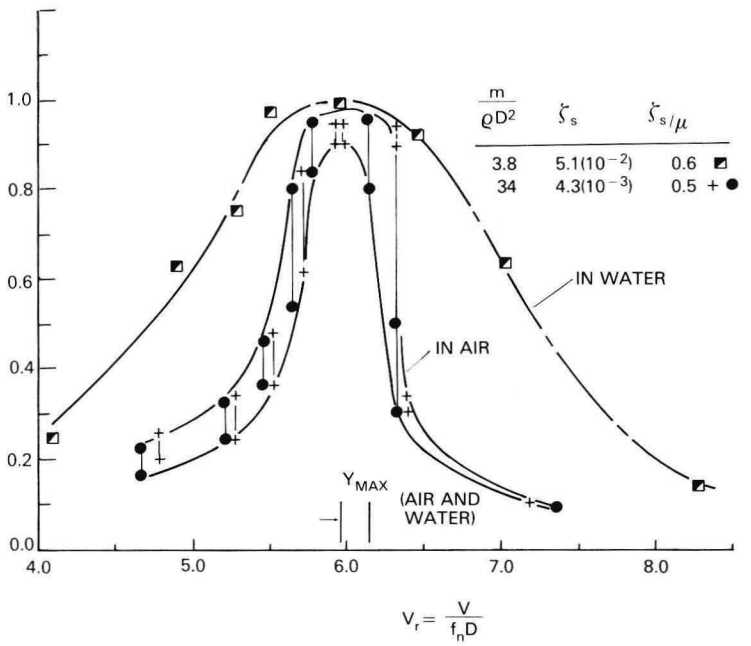

Fig. 1 — The cross flow displacement amplitude, $2\bar{Y}/D$, for a circular cylinder plotted against the reduced velocity, $V_r = V/f_nD$, from Ref. (5).

The value of V_r^{-1} at the peak amplitude of displacement yields a Strouhal number of $St \sim 0.17$. This is because the oscillation (and vortex shedding) frequency at resonance is about $f = 0.8$ to $0.85\ f_s$ at the flow velocity V corresponding to $\bar{Y}_{MAX}$.

The narrow resonance band in air is typical of lightly-damped systems while the more broad resonance in water is typical of systems with relatively higher structural damping. It can be seen that even though the damping and mass ratios of the two systems differ by factors of ten, the *reduced damping* (the product of the mass ratio $m/\rho D^2$ and the structural damping ratio ζ_s) is very nearly the same and so are the peak displacement amplitudes for the two cases. This overall pattern of behavior is typical of measurements in water and in air at all Reynolds numbers where vortex shedding takes place.

It has been shown by numerous investigators that the displacement amplitude is a function primarily of a response or "reduced damping" parameter of the form

$$k_s = \frac{2m\delta}{\rho D^2}. \tag{1}$$

The reduced damping can be written in the analogous form

$$\zeta_s/\mu = 2\pi\ St^2 k_s \tag{2}$$

when the damping is small and $\zeta_s = \delta/2\pi$. Here μ is an expression of the mass ratio. The importance of the reduced damping follows directly from resonant force and energy balances on the vibrating structure. It is important to note that the damping coefficients ζ_s and δ represent the damping measured in *still air*. For all practical purposes this is then equivalent to in vacuo structural damping. Moreover, the relation between Y_{MAX} and k_s or ζ_s/μ holds equally well for flexible cylindrical members with normal mode shapes given by $\psi_i(z)$, for the i th mode.

If the cross flow displacement (from equilibrium) of a flexible structure with normal modes $\psi_i(z)$ is written as

$$y_i = Y\psi_i(z) \sin \omega t \tag{3}$$

at each spanwise location z, then the peak displacement is scaled by the factor

$$Y_{EFF,MAX} = Y_{MAX} I_i^{1/2} / |\psi_i(z)|_{MAX} = Y_{MAX}/\gamma_i, \quad Y = \bar{Y}/D, \tag{4a}$$

where

$$I_i = \frac{\int_0^L \psi_i^4(z)\, dz}{\int_0^L \psi_i^2(z)\, dz}, \tag{4b}$$

and

$$\gamma_i = \frac{|\psi i(z)|_{MAX}}{I_i^{1/2}}. \tag{4c}$$

The effective displacement amplitude Y_{EFF} is a scaled version of the displacement amplitude $\bar{Y}_{MAX}$ which is derived from considerations based on several versions of the so-called "wake oscillator" approach to modelling vortex-excited oscillations [12,13].

Experimental data for Y_{EFF} as a function of ζ_s/μ are plotted in Fig. 2. These results encompass a wide range of single cylinders of various configurations and flexure conditions at Reynolds numbers from 300 to 10^6. For *all* of the data points plotted in Fig. 2 the damping coefficients ζ_s and/or δ were measured in *still* air. This should minimize any further misconceptions among other investigators who have discussed various versions of this figure. The various types of structures represented by the data points available through 1982 are given by Griffin and Ramberg [5]. As a typical example, the deflections of a flexible cantilever in the fundamental mode have been measured under a variety of conditions. Peak-to-peak displacements as great as two to four diameters in water were measured for length/diameter ratios up to about 250. All available experiments conducted to date indicate that the limiting unsteady displacement amplitude for a flexible circular cylinder is about $Y_{EFF} = \pm$ 1 to 1.5 at the lowest values of reduced damping.

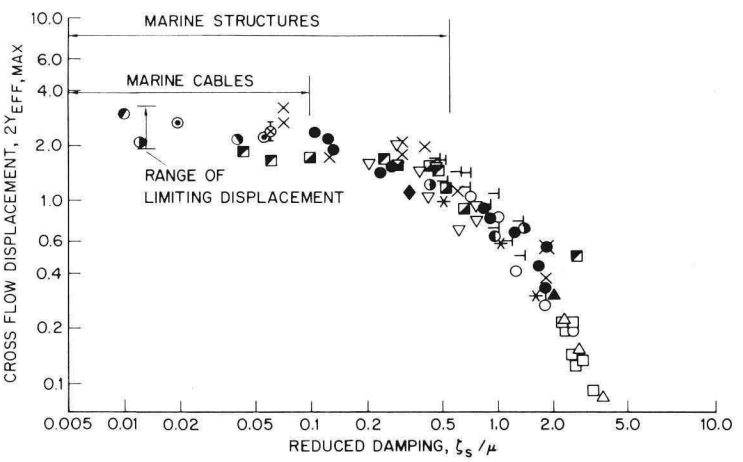

Fig. 2 — The maximum peak-to-peak cross flow displacement amplitude, $2Y_{EFF,MAX}$, of circular cylinders, scaled as in Eq. (4), as a function of the reduced damping, $\zeta_s = 2\pi St^2 k_s$. The complete legend for the data points is given in Ref. (5), except for the recent data of Moe (1982), ⊙ and of Every and King (1974), ○.

The most recent measurements in water shown in Fig. 2 have been provided by Every and King [14] and by Moe [15] and are given by the symbols ○ and ⊙ respectively. Both provide additional confirmation of the earlier trends shown in the figure. It is interesting to note that the reduced damping can increase from $\zeta_s/\mu = 0.01$ to 0.5 (a factor of *fifty*) and the displacement amplitude decreases only from two or three diameters to one diameter (a nominal factor of only *two or three*). This is why it is difficult to suppress the in-water oscillations by means of mass and damping control. Recent discussions of the suppression of vortex-excited oscillations in water are given by Every, King and Griffin [14,16] and by Zdravkovich [17].

The situation is somewhat different in air as shown in Fig. 3, which has been adapted from Adami and Batch [8]. The vibrations of a model bus-bar ($L/D = 114$) were measured in a wind tunnel with different end fixities. For the conditions tested the vibrations were nearly independent of the mode, end conditions and the aspect ratio [8]. The solid line in the figure is the prediction [18]

$$\bar{Y}_{MAX}/D = \frac{1.29\,\gamma_i}{[1 + 0.43\,(4\pi\ St^2 m\delta/\rho D^2)]^{3.35}}. \tag{5}$$

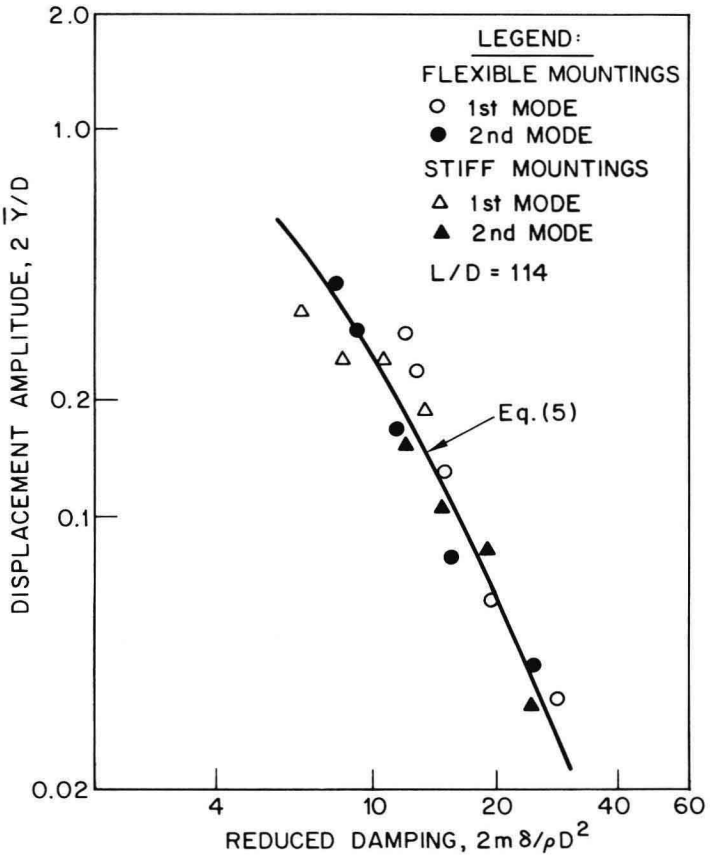

Fig. 3 — The cross flow peak-to-peak displacement amplitude, $2\bar{Y}/D$, for flexible circular cylinders in a wind tunnel as a function of the reduced damping, $k_s = 2m\delta/\rho D^2$; adapted from Adami and Batch (1981).

This is a least-squares fit to the data in Fig. 2 which were available in 1977. Other virtually identical prediction curves derived by different methods have been proposed by Sarpkaya [1] and Blevins [19]. The various approaches taken are discussed by Paidoussis [9]. The data plotted in Fig. 3 are typical of those obtained in air and would fall toward the right-hand side of Fig. 2. In that region the displacement amplitude is strongly dependent on the reduced damping. Control of the mass and damping of the member then provides a means for suppressing the vibrations.

These results have been obtained both in air and in water, even though the mass ratios of vibrating structures on the two media differ by two orders of magnitude. For typical structures vibrating in water the mass ratio $\frac{m}{\rho D^2}$ varies from slightly greater than 1 to about 5; in air the mass ratios corresponding to Fig. 2 typically vary from $\frac{m}{\rho D^2} = 15$ to 500.

LIFT FORCES

When a cylindrical body resonantly vibrates due to vortex shedding, the periodic motion is accompanied by increased coherence of the vortex shedding spanwise along the body and by an amplification of the unsteady fluid forces. Although some measurements of the forces have been made, only recently has attention been given to understanding the mechanisms by which this fluid-structural interaction force is generated and how the fluid forces may be scaled with some confidence to large Reynolds numbers.

The total fluid force which acts on a resonantly vibrating, cylindrical structure due to vortex shedding can be divided into several components [20,21], which are:

- An exciting force component, by which energy is transferred to the structure;
- A reaction, or damping force, which is exactly out-of-phase with the structure's velocity;
- An "added mass" force, which is exactly out-of-phase with the structure's acceleration; and
- A flow-induced inertial force.

These various components can be deduced from the total hydrodynamic force as measured, say, by Sarpkaya [1] or the various components can be measured individually as was done by Griffin and Koopmann [10], for example. The present discussion will deal essentially with the exciting force.

The excitation component of the total unsteady hydrodynamic force is defined as

$$C_{LE} = C_L \sin \phi \tag{6}$$

and is important because it is the component of the total force that transfers energy to the vibrating structure. Here ϕ is the phase angle between the hydrodynamic force coefficient C_L and the motion of the structure. A relatively large number of measurements of C_{LE} by various means are plotted against the effective displacement amplitude Y_{EFF} in Fig. 4. Table 1 describes the various conditions under which the experimental results were obtained. Several important characteristics of the unsteady lift and pressure forces that accompany vortex-excited oscillations are clear from the results. First there is a maximum of the excitation force coefficient at a peak-to-peak displacement amplitude of between 0.6 and 1 diameters for all the cases shown in the figure. Second, the maximum of the force coefficient is approximately $C_{LE} = 0.5$ to 0.6 for all but one case; the exception is the single result of $C_{LE} = 0.75$. C_{LE} then decreases toward zero and results in a limiting effective displacement amplitude between two to three diameters. This limiting amplitude is clearly shown at the low values of reduced damping in Fig. 2. Similar behavior in the pressure coefficient measured near the separation point on a forced-vibrating cylinder was obtained by Bearman and Currie [22].

Vortex-induced vibrations cause energy to be transferred to the cylindrical structure. This is caused at resonance by the excitation force component plotted in Fig. 4. A number of measurements of aerodynamic power have been made, primarily in the study of electrical transmission line vibrations; see, for example, the paper by Simmons and Cleary [6]. The time-averaged power input $\bar{P}$ over a cycle of the oscillation is

$$\bar{P} = \pi f \bar{F}_L \bar{Y} \sin \phi \tag{7}$$

when the displacement of the cylinder is

$$\bar{y}(t) = \bar{Y} \cos 2\pi ft \tag{8a}$$

and the lift force is

$$\bar{F}(t) = \bar{F}_L \cos (2\pi ft + \phi). \tag{8b}$$

In nondimensional terms Eq. (7) reduces to

$$P = \frac{\bar{P}}{\rho D^4 f^3} = \frac{\pi}{2} Y C_L \sin \phi V_r^2 \tag{9a}$$

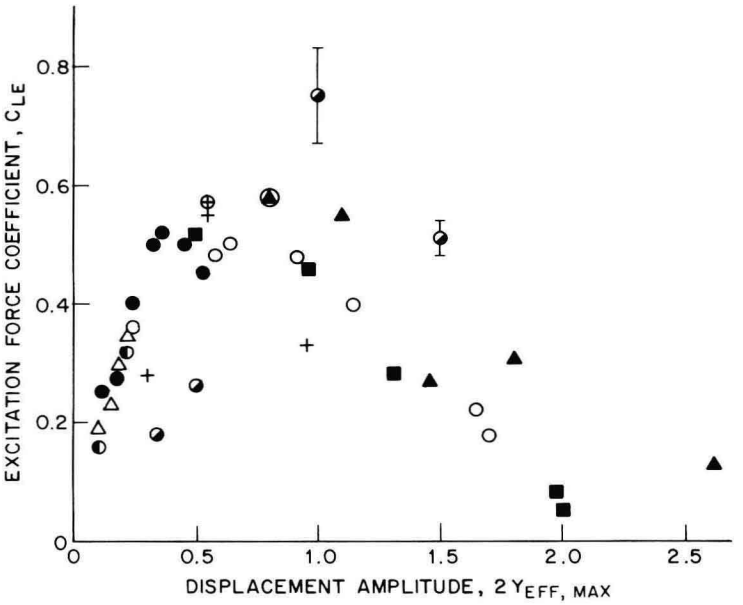

Fig. 4 — The excitation component, C_{LE}, of the lift force plotted against the displacement amplitude $2Y_{EFF,MAX}$, scaled as in Eq. (4). The legend for the data points is given in Table 1.

Table 1
The Excitation Force Coefficients on Vibrating Bluff Cylinders; Description of the Data in Fig. 4

Symbol	Type of cylinder	Medium	Cylinder material	Investigator(s)
▲	Flexible cantilever	Water	PVC	King (1977)
■			PVC	
			Aluminum	
			Stainless steel	
○	Pivoted rigid cylinder	Water & Air	Brass	Vickery and Watkins (1964)
+	Spring-mounted rigid cylinder	Air	Aluminum tubing	Griffin and Koopmann (1977)
◒	Rigid cylinder, forced oscillations	Water	Aluminum tubing	Sarpkaya (1978)
Δ	Flexible cantilever	Air	Aluminum	Hartlen, Baines and Currie (1968)
●	Flexible cylinder	Air	—	Farquharson and McHugh (1956)†
◐	Rigid cylinder, forced oscillations	Air	Brass	Simmons and Cleary (1979)

†Quoted by Simmons and Cleary.

or, equivalently,

$$P = \frac{\pi}{2} Y C_{LE} V_r^2. \tag{9b}$$

Several examples of the measured and predicted time-average power P are given in Fig. 5. The measured values are from Simmons and Cleary and from Farquharson and McHugh. The latter examples were reduced by Simmons and Clearly from Ref. (23). The measured and predicted values are virtually indistinguishable for the case $V_r = 6$. The predictions of P are based upon a least-squares fit to the data in Fig. 4. As shown in Fig. 1 this condition is representative of the maximum power transmission in both air and water. The example given here is for the case of a vibrating transmission line in air, but a similar approach could be used to predict the hydrodynamic power transmission to and acoustic radiation from an oscillating member in water.

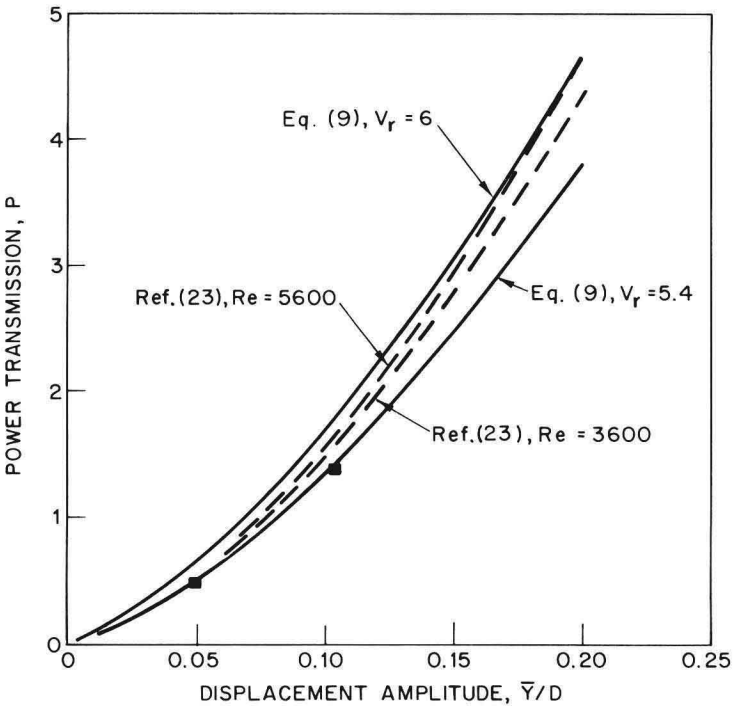

Fig. 5 — The measured and predicted time-averaged power transmission, P, to a vibrating circular cylinder plotted against the displacement amplitude, $\bar{Y}/D$. — — — —, Farquharson and McHugh (1956), from Simmons and Cleary (1979); ■, Simmons and Cleary (1979).

DRAG FORCES

An important consequence of the resonant cross flow oscillations of structures and cables due to vortex shedding is an amplification of the steady drag force (or equivalently the drag force coefficient C_D). The drag amplification under a variety of conditions has been measured and the results have been summarized by Griffin and Ramberg [5]. A step-by-step method for employing these measurements in the analysis of marine cable structures was developed by Skop, Griffin and Ramberg [18]. One step in the method uses Eq. (5) to predict the cross flow displacement amplitude of the member. This procedure has been extended to the case of flexible, cylindrical marine structures by Griffin [4] in a study of OTEC cold water pipe vibrations. Measurements of the drag coefficient more recent than those discussed by Griffin and Ramberg are presented here.

Measurements of the vortex-induced cross flow vibrations of model marine piles were made by Fischer, Jones and King [26,27]. The steady deflection at the free end of the model pile also was measured; in this case the model was a simple, uniform cantilever beam with no tip masses, fully immersed in water, and normal to the incident flow. For low flow velocities the measured and predicted tip deflections coincided when the pile was effectively stationary. The deflection was predicted by assuming a uniform loading function

$$w(x) = 1/2\ \rho V^2 D C_D(x)$$

over the length of the flexible beam in which the drag coefficient $C_D(x)$ was a constant, $C_D = 1.2$.

When the critical flow velocity for the onset of the vortex-induced vibrations was exceeded, the measured steady deflections in line with the flow departed significantly from the predicted reference curve. One example of the results obtained is given in Fig. 6. For the lower values of relative density the flow velocities above the threshold value caused steady deflections of up to twice the model's value predicted by assuming $C_D = 1.2$. For the higher values of relative density, the steady deflections of the model diverged from the predicted curve, reached a maximum as shown in Fig. 6, and then returned to the predicted curve as the flow velocity was increased still further. The region of divergence corresponds directly to the range of resonant, large amplitude cross flow vibrations. For example, the tip of the $SG = 3.5$ pile was deflected in line about 1.3 diameters at a water velocity V of 0.6 kt (0.3 m/s). At this same flow velocity the cross flow displacement amplitude was ± 1.5 diameters. When the pile was restrained from oscillating, the steady in-line deflection of the tip was predicted to be 0.6 diameters at the same flow velocity. The predicted tip deflections in Fig. 6 were computed using an approach which is discussed by Every, King and Griffin [16].

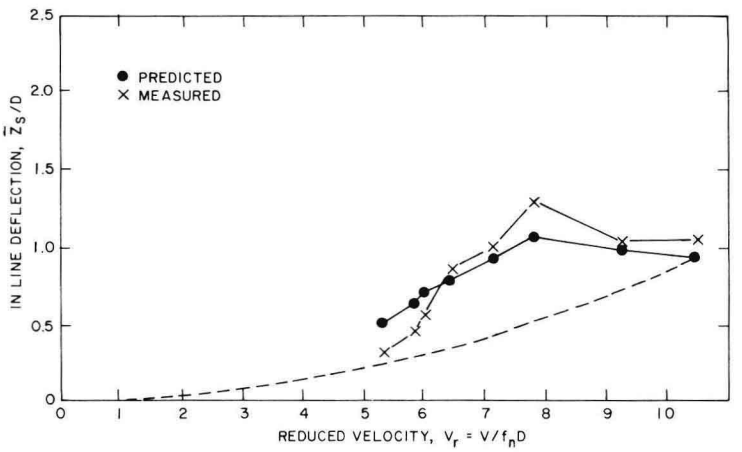

Fig. 6 — The predicted and measured steady tip deflection, $\bar{z}_s/D$, for a vibrating flexible cantilever in water; from Every, King and Griffin (1982). Relative density of the beam, SG = 3.5; — — — — —, beam restrained from oscillating, $C_{D0} = 1.2$.

The mean vortex-induced drag coefficient C_D on a freely-oscillating, spring-mounted cylinder is plotted against the reduced velocity V_r in Fig. 7. The measurements were made by Overvik [28] as a baseline case in a more extensive study of the effects of vortex shedding on marine risers. The drag on the cylinder clearly undergoes a resonant-like behavior in much the same manner as the cross flow displacement amplitude. Comparable measurements by Overrik of the displacement amplitude $\bar{Y}/D$ correspond directly with the behavior of the drag coefficient C_D. At the peak value of the response, $\bar{Y} \sim 1.1\ D$, the drag coefficient on the vibrating cylinder is $C_D = 2.5$. This is an amplification of about 250 percent, which is of sufficient magnitude to cause serious problems for the designer of marine structural members of cylindrical cross section. Less severe problems develop in the case of structures in air because of the smaller vibration amplitudes which are common there.

The drag amplification C_D/D_{D0}, where C_{D0} is the drag coefficient for the stationary cylinder, from a variety of recent experiments is plotted in Fig. 8 as a function of the "wake response" parameter

$$w_r = (1 + 2\ \bar{Y}/D)\ (V_r St)^{-1}. \tag{10}$$

This parameter was introduced by Skop, Griffin and Ramberg [18] as a means for correlating the drag amplification that accompanies vortex-induced vibrations. In the particular form shown the factor St^{-1} acts

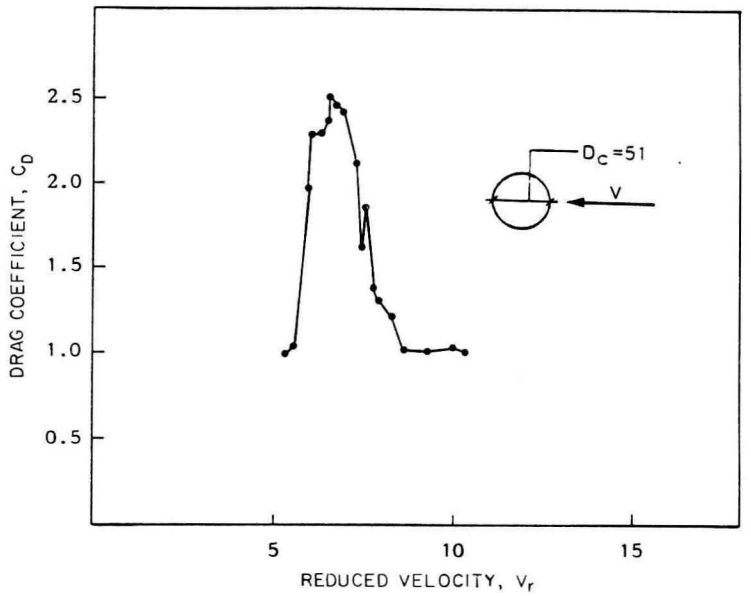

Fig. 7 — The drag coefficient, C_D, plotted against the reduced velocity, V_r, for a spring-mounted circular cylinder; from Overvik (1982). Peak cross flow displacement amplitude, $\bar{Y} = \pm$ 1 to 1.1D.

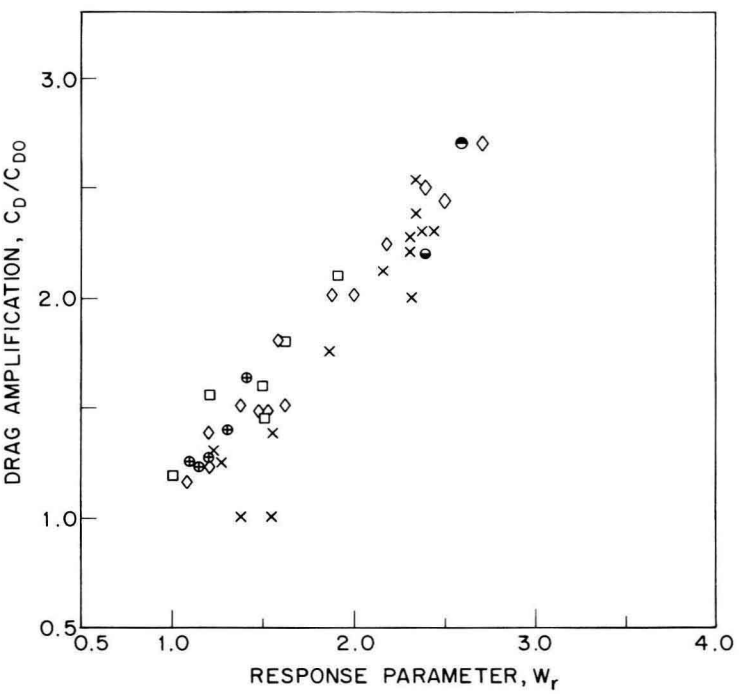

Fig. 8 — The drag coefficient amplification, C_D/C_{D0}, plotted as a function of the wake response parameter, $w_r = (1 + 2\bar{Y}/D)\ (St\ V_r)^{-1}$, for the cross flow vibrations of a circular cylinder. The legend for the data points is given in Table 2.

Table 2
Drag Force Amplification on Vibrating Circular Cylinders; Description of the Data in Fig. 8

Symbol	Medium	Type of Vibration	Investigator(s)
⊕	Air	Cross flow, forced	Griffin and Ramberg (1975)
Δ	Water	Cross flow, forced	Sarpkaya (1977)
□	Water	Cross flow, forced	Schargel (1980)
X	Water	Cross flow, free	Overvik (1982)
◓, ◒	Water	Cross flow, free	Moe (1982)

to correct for any variations in Strouhal number (and Reynolds number) among the various sets of data. All of the data in Fig. 8 refer to conditions of lock-in between the vortex and vibration frequencies. A previous drag amplification-wake response plot was used by Every, King and Griffin [16] for the predictions shown in Fig. 6.

It is interesting to note the variety of data which are correlated in the figure. For instance, the drag coefficients from Griffin and Ramberg [29] were derived from wake measurements with a forced-vibrating cylinder in air. The drag measurements from Sarpkaya [30] and Schargel [31] were made on a forced-vibrating cylinder in water. Moe [15] and Overvik [28] measured the drag on a freely-vibrating cylinder in water. All of these different experiments resulted in substantial amplifications of the drag coefficient, with $C_D/C_{D0} > 2$ not uncommon for both free and forced vibrations in water.

Similar levels of hydrodynamic drag amplification were measured during the recent field experiments reported by Vandiver and Griffin [32,33]. Both a 23 m(75 ft) long pipe and a cable with and without attached masses underwent large-amplitude vibrations ($\bar{Y} \sim \pm 1D$) due to vortex shedding in a steady current. Mean drag coefficients of $C_D = 2.4$ to 3.2 were measured during the time intervals when the pipe and cable were oscillating at these large amplitudes. In another recent series of experiments Davies and Daniel [34] measured the strumming vibrations of submersible umbilical cables. The model cable of L/D = 100 to 300, which was tested in a large water channel, consistently was excited into large-amplitude cross flow oscillations which were comparable in level to those reported by Vandiver and Griffin. Consequently the normal mean drag coefficients measured by Davies and Daniel were in the range $C_D = 2.5$ to 3.4. This is an amplification factor of 2 to 2.8.

The overall implications for practical applications are that the relatively large amplitudes of vibration caused by vortex shedding, and the amplifications of the unsteady and steady fluid forces which are a consequence of the vibrations, can cause both large steady deflections and stresses and time dependent, fatigue-related unsteady forces and stresses.

SUMMARY AND CONCLUDING REMARKS

Until recent years problems associated with vortex shedding were given scant attention or approached on an ad hoc case-by-case basis, largely because reliable experimental data and design procedures were not available for general use. However, the dynamic analysis of modern structures and cable systems has become increasingly important and modern in order to predict stress distributions and operational lifetimes in hostile environments. This is largely because the amplitudes of vibration for a cylindrical structure such as a riser or pipeline in water are an order of magnitude greater than for a similar structure in air. The small mass ratio (structure to displaced fluid) in water produces small values of the reduced damping which in turn result in the relatively large vibration amplitudes shown here in Fig. 2.

There is a large range of reduced damping over which bluff cylindrical structures in water undergo large-amplitude vibrations due to vortex shedding. Thus it is not possible to suppress these oscillations by means of mass and damping control, and some form of external device such as a helical strake winding or fairing is required. The component of the lift coefficient which drives the motion is increased by vibration, as is the mean in-line drag coefficient which is increased by as much as 250 percent.